Dalton Transactions

ROYAL SOCIETY OF CHEMISTRY

PAPER

View Article Online
View Journal | View Issue

Cite this: *Dalton Trans.*, 2026, **55**, 3120

Boronate esters for the binding and detection of low molecular weight volatile amines

Xiaoning Li,[a] James Boyt,[b] Min Cai,[b] Steven Sloope,[b] Luke T. Lackovic,[b] Mark D. Smith [b] and John J. Lavigne *[b]

Received 17th November 2025,
Accepted 21st January 2026

DOI: 10.1039/d5dt02760h

rsc.li/dalton

Conjugated thiophene-based diboronate esters, **1–4**, were synthesized to investigate how substituents on catechol alter the Lewis acidity and accessibility to boron, and influence binding interactions with low molecular weight Lewis basic amines. Crystallographic analysis indicated that both boron centres bind analyte and that Lewis base coordination induces deplanarization of the conjugated system. Spectroscopic studies demonstrate that amine binding disrupts conjugation, producing distinct and reproducible optical responses that depend on analyte basicity and structure, with association constants in organic solvent ranging from 10^3 to 10^6 M^{-1}. Quantitative binding analyses indicate strong negative cooperativity between the two boron sites. These results establish design principles for cross-reactive optical sensor arrays capable of differentiating volatile amines relevant to environmental monitoring, food quality assessment, and biomedical diagnostics.

Introduction

Conjugated organic materials have drawn attention for their many applications as dyes,[1] sensors,[2] and field effect transistors.[3] The incorporation of electron rich and electron deficient groups is commonly used to modulate the electronic properties of the resulting products by adjusting the HOMO–LUMO band gap.[4,5] Boron containing materials, specifically boranes, have been studied extensively as the low-lying empty p-orbital on the boron provides a conjugated bridge between aromatic residues. Despite being structurally similar, borinic and boronic ester-based compounds have been largely overlooked. We previously demonstrated that there is conjugation through the borole linkage in oligo and poly(boronic esters).[6,7] This is utilized in the development of chemical sensors, as Lewis base binding to the boron disrupts conjugation, leading to changes in the absorption and emission properties.[8,9] To further understand how substituents impact interactions at the boron centres, we present here a study of the binding of low molecular weight volatile amines to a series of thiophene-diboronic esters.

These studies address a need to understand how these small organic molecules can bind to analytes of biological and environmental relevance. Volatile amines are common pollutants from agriculture and the chemical and pharmaceutical industries due to extensive use in fertilizers, colorants and medicines,[10,11] as well as being indicators of quality in foods.[12–15] In certain diseases, volatile amines also serve as biomarkers for medical diagnoses.[16] Thus, a readily synthesized optical sensor for the detection of volatile amines could be utilized for pollution control, food quality evaluation and medical diagnoses. State-of-the-art detection methods for volatile amines include electrochemical analysis,[17] as well as gas[18] and liquid chromatographic methods.[19,20] However, these detection methods tend to be time-consuming and require high-cost instruments and highly trained operators. Consequently, recent efforts have addressed the desire for rapid, straightforward and low-cost detection methods.

Optical sensing materials for volatile amine detection based on electrostatics,[21,22] hydrogen bonding[23,24] and Lewis acid–base interactions[25–27] have been developed, including conjugated organoboranes.[28–31] As an alternative to organoboranes, boronic esters display enhanced planarity through the borole linkage and reduced steric interactions with potential guests,[7,32] and have been used to bind ions.[33–35] Furthermore, this B–N bonding interaction has been useful in the development of supramolecular materials with unique structural, electronic, and "self-healing" properties.[36]

The investigations presented herein use a series of diboronate esters (Scheme 1) capable of differentially binding low molecular weight amines to probe the mechanism by which analyte is bound and an optical signal is generated. The elec-

[a]*Department of Chemistry, Georgia Southern University, Statesboro, GA 30460, USA. E-mail: xiaoningli@georgiasouthern.edu*
[b]*Department of Chemistry & Biochemistry, University of South Carolina, Columbia, SC 29208, USA. E-mail: Lavigne@sc.edu; Fax: +01 803 777 9521; Tel: +01 803 777 2295*

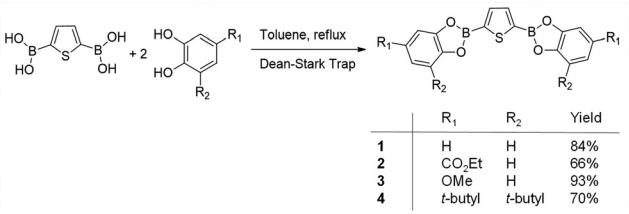

	R_1	R_2	Yield
1	H	H	84%
2	CO_2Et	H	66%
3	OMe	H	93%
4	*t*-butyl	*t*-butyl	70%

Scheme 1 Synthesis of thiophene bis(dioxaborole)s (**1–4**).

tronic properties and accessibility to the analyte binding site on boron are controlled without disrupting π-conjugation by varying the substituents on the aromatic diol moiety.[6]

Experimental section

General

Solution phase ^{1}H NMR and ^{13}C NMR, and ^{11}B NMR spectra were collected on a Bruker Avance III-HD (300 MHz for ^{1}H and 400 mHz for ^{11}B and ^{13}C). UV-vis absorbance studies were performed using a Beckman Coulter DU 640 Spectrophotometer and quartz cuvettes from Starna. Fluorescence emission studies were performed using a Cary Eclipse Fluorescence Spectrophotometer. X-ray diffraction data was collected at Bruker SMART APEX diffractometer Mo Kα radiation. 3-Methoxycatechol was obtained according to a literature procedure.[37] Chemicals for all syntheses were purchased from Acros and Sigma-Aldrich and used without further purification. All solvents were obtained from solvent purification systems from Innovative Technologies. Note that in the ^{13}C NMR data provided for the compounds below, the signal for the carbon directly attached to the boron is not observed due to the quadrupolar splitting from the boron.

Synthesis and characterization

Compound 1. To a mixture of 2,5-thiophenediboronic (350 mg, 2 mmol) and catechol (529 mg, 4.8 mmol) 50 ml of dry toluene was added. The solution was heated to reflux under a nitrogen atmosphere with Dean–Stark trap for 16 hours. The clear solution was cooled to room temperature and solvent was removed by rotary evaporation. The excess catechol was removed by a Kugel-Rohr at 95–100 °C under reduced pressure (0.1 Torr) for 5 hours. White powder (270 mg, 84%) was obtained. ^{1}H NMR (300 MHz, $CDCl_3$): δ 8.08 (s, 2H), 7.34 (m, 4H), 7.16 (m, 4H); ^{13}C NMR (100 MHz, $CDCl_3$): δ 148.2, 139.5, 123.1, 112.7, 105.0; ^{11}B NMR (128.42 MHz, $CDCl_3$, $BF_3{\cdot}Et_2O$ = 0 ppm as the external reference and boric acid as the second reference at 19.3 ppm): δ 29.6; HR-MS: cacld for $C_{16}H_{10}B_2O_4S$: 320.0492, found, *m*/*z* 320.0493; *E* = 0.3 ppm.

Compound 2. A mixture of 2,5-thiophenediboronic (50.2 mg, 0.29 mmol) and ethyl-3,4-dihydroxybenzoate (106.2 mg, 0.58 mmol) was refluxed in 30 mL toluene. Using the procedures described above, a white powder was obtained as the final product (85.6 mg, 65.9%). ^{1}H NMR (300 MHz, $CDCl_3$): δ 8.11 (s, 2H), 8.02 (d, *J* = 1.5 Hz, 2H), 7.97 (q, 2H), 7.37 (d, *J* = 8.1 Hz, 2H), 4.41 (q, 4H, CH_2), 1.02 (t, 12H, Me); ^{13}C NMR (100 MHz, $CDCl_3$): δ 166.0, 151.8, 148.0, 140.0, 126.0, 125.8, 114.0, 112.3, 61.2, 14.3; HR-MS: cacld for $C_{22}H_{18}B_2O_8S$: 464.0917; found, *m*/*z* 464.0912; *E* = 1.1 ppm.

Compound 3. A mixture of 2,5-thiophenediboronic (68.9 mg, 0.40 mmol) and 4-methoxycatechol (123.6 mg, 0.88 mmol) was refluxed in 30 mL toluene. Using the procedures described above, a gray powder was obtained as final product (141.8 mg, 93.3%). ^{1}H NMR (300 MHz, $CDCl_3$): δ 8.05 (s, 2H), 7.21 (d, *J* = 9.0 Hz, 2H), 6.94 (d, *J* = 3.0 Hz, 2H); 6.69 (dd, *J* = 3.0 Hz, 2H); 3.83 (s, 6H, OMe) ^{13}C NMR (100 MHz, $CDCl_3$): δ 156.1, 149.1, 142.5, 134.4, 112.1, 108.0, 99.7, 56.1; HR-MS: cacld for $C_{18}H_{14}B_2O_6S$: 380.0704; found, *m*/*z* 380.0712; *E* = 2.1 ppm.

Compound 4. A mixture of 2,5-thiophenediboronic (50.0 mg, 0.29 mmol) and 3,5-di-*tert*-butylcatechol (142.4 mg, 0.64 mmol) was refluxed in 50 mL toluene. Using the procedures described above, a white powder was obtained as final product (111 mg, 70%).^{1}H NMR (300 MHz, CD_2Cl_2): δ 8.08 (s, 2H), 7.26 (d, *J* = 1.2 Hz, 2H), 7.14 (d, *J* = 1.5 Hz, 2H), 1.52 (s, 18H, Me), 1.36 (s, 18H, Me); ^{13}C NMR (100 MHz, $CDCl_3$): δ 148.1, 146.1, 143.8, 139.0, 135.1, 116.8, 107.7, 35.0, 34.5, 31.9, 31.8, 29.8; HR-MS: cacld for $C_{32}H_{42}B_2O_4S$: 544.3001; found, *m*/*z* 544.3000; *E* = 0.2 ppm.

^{1}H-NMR measurements

Spectra were collected of (1) a 20 mM solution of compound **1** in dry $CDCl_3$; (2) a solution of 20 mM **1** and 40 mM of TBAF in dry $CDCl_3$ (Fig. 1); and (3) a solution of 20 mM **1** and 40 mM of nBuNH$_2$ in dry $CDCl_3$. To this final solution, 6 μL of trifluoroacetic acid (~80 mM) was added. The sample was shaken for 1 min and then the spectrum collected (Fig. 3).

Absorbance titrations

A 4 mM stock solution of **1** was prepared in dry dichloromethane. The stock solution was diluted to 0.035 mM working solution with dichloromethane for the titration studies using nBuNH$_2$, iPrNH$_2$ and iPr$_2$NH. The working solution for sensor

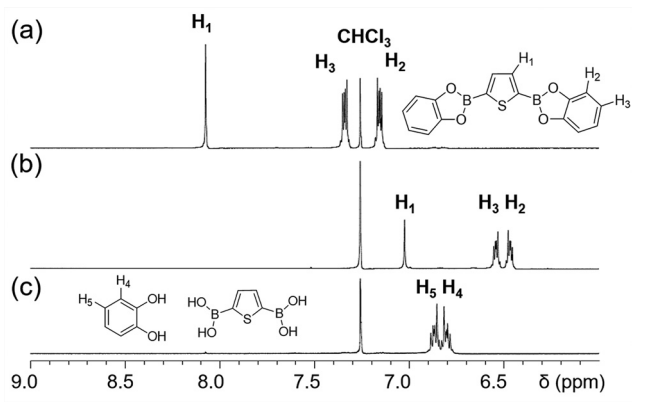

Fig. 1 ^{1}H NMR spectra ($CDCl_3$) of (a) **1** (20 mM), (b) **1** (20 mM) with 2 equiv. fluoride (40 mM), and (c) a mixture of 2,5-thiophene diboronic acid (20 mM) and catechol (40 mM).

1 was prepared at 0.02 mM from the same stock solution for titrations with iPr_2EtN and TBAF. Stock solutions (100 mM) for each amine analyte and fluoride ion were made in dry dichloromethane. The solution was diluted to 10 mM for $nBuNH_2$, $iPrNH_2$ and iPr_2NH, and to 5 mM for iPr_2EtN and TBAF as analyte working solutions for titrations. The sensor stock solutions for compound **2–4** were prepared by the same procedures for the absorption titration studies.

A sealed quartz cuvette was charged with 2 mL of the sensor working solution and the absorbance spectrum acquired at 25 °C. An absorption scan was taken after each addition of 1 or 2 μL of the analyte working solution in an air/moisture free manner (*i.e.*, *via* syringe through a septum sealed cuvette). Three replicates were produced for each titration.

X-ray crystal structure determination

A solution of compound **1** (20 mM) was made in dry benzene. White crystals of **1** were obtained from slow evaporation of benzene after approximately 72 h. White crystals of **1**–2F were obtained from the slow evaporation of a mixture of compound **1** (20 mM) and two equivalent of tetra-*n*-butylammonium fluoride (TBAF) in $CDCl_3$ after approximately 48 h.

Results and discussion

Synthesis

Thiophene containing conjugated bis(dioxaborole)s **1–4** were investigated due to the coupling of the electron-rich heteroaromatic ring[28,38,39] with the electron deficient boroles. This type of donor–acceptor system has demonstrated efficient optical transitions upon perturbation of the pi-system.

The desired boronates were synthesized by condensing 2,5-thiophenediboronic acid and the appropriate aromatic diol in 65–95% yield (Scheme 1). To assess the factors affecting binding of amine analytes with compounds **1–4**, electron-donating (–OMe, **3**), electron-withdrawing (–CO_2Et, **2**) and sterically incumbered (–di-*t*Bu, **4**) substituents were incorporated on the aromatic diol component, providing diboronic esters with altered Lewis acidity and steric hindrance. Moreover, volatile amines with varying sterics and basicities/nucleophilicities were chosen to investigate the impact analyte structure has on binding and signal generation.

Fluoride ion binding

Fluoride ion was used as a model Lewis base to probe the binding interaction with the Lewis acidic boron centres in the bis(dioxaborole)s. Using ^{1}H NMR, resonances for the aromatic protons of **1** (Fig. 1a) shifted upfield after the addition of fluoride from TBAF (Fig. 1b) due to increased shielding in the **1**-fluoride complex. Investigations of the binding stoichiometry suggested that each boron atom can interact with one fluoride ion, affording a 1 : 2 bis(dioxaborole) to fluoride ratio (Fig. S35).[40] Moreover, no resonances were observed for starting materials upon fluoride addition (Fig. 1b *vs.* c) indicating the stability of the ester upon binding analyte.[41] To demonstrate the reversibility of this interaction, TMS-Cl was added to the **1**-F complex to successfully compete for the fluoride, regenerating free host **1** (Fig. S2). Similarly, ^{11}B NMR of **1** showed a single broad peak centred at 29.6 ppm,[42] indicative of sp^2 hybridized trigonal planar boron such as that found in the ester. Upon addition of 2 equivalents of TBAF (1 : 1 B : F ratio) the resonance shifted upfield to 8.0 ppm suggesting a clean change in hybridization at the boron to sp^3. Once TMS-Cl was added, the boron signal returned to that of unbound sp^2 hybridized **1** at 29.6 ppm (Fig. S3). Analogous ^{19}F NMR studies further support the complete coordination of this anion with boron (Fig. S4).

The solid-state structures of **1** and **1**–2F, determined from single crystal XRD (Fig. 2a and b), reveal the predicted trigonal planar geometry around both boron centres in **1**, with the ring dihedral angles deviating only 1–10° from planarity, implying near-ideal conjugation (Table 1). In contrast, conventional boranes exhibit dihedral angles from 30°–90° depending on the boron-substituents.[43–45] The X-ray data for the **1**–2F complex shows the deplanarization of the bis(dioxaborole) after formation of the boron-fluorine bonds, thus disrupting conjugation.

While fluoride provides mechanistic insight, our objective was to bind weaker Lewis bases, *e.g.* amines. As a typical example we used *n*-butylamine ($nBuNH_2$). The aromatic proton resonances of **1** shifted upfield upon addition of 2 equivalents of $nBuNH_2$ (Fig. 3a and b), though not as significantly as when fluoride was added (Fig. 1b). The broad resonances depicted in Fig. 3b are due to signal averaging upon fast exchange between free and bound amine. As expected, the interaction between **1** and $nBuNH_2$ was weaker than that between **1** and fluoride, redu-

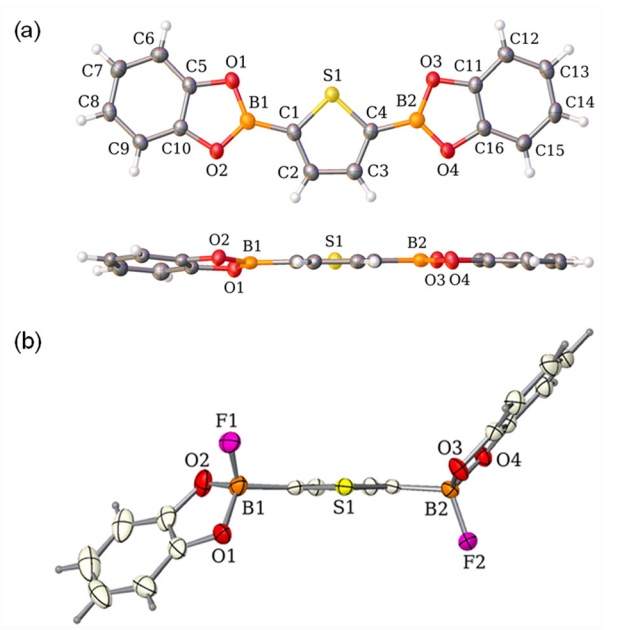

Fig. 2 Solid state structures of **1** (a) and **1**–2F (b). Displacement ellipsoids at 60% probability level. Counterions and solvent omitted for clarity.

Table 1 Selected bond lengths, (dihedral) angles of **1** and **1**–2F

Compd	Bond length/Å	Bond angle/°	Dihedral angle
1	B(1)–O(1) 1.384(2) B(1)–O(2) 1.387(2) B(1)–C(1) 1.537(2) B(2)–O(4) 1.386(2) B(2)–O(3) 1.387(2) B(2)–C(4) 1.533(2)	O(1)–B(1)–O(2) 112.14(15) O(1)–B(1)–C(1) 124.83(15) O(2)–B(1)–C(1) 123.03(15) O(4)–B(2)–O(3) 112.16(14) O(4)–B(2)–C(4) 122.24(15) O(3)–B(2)–C(4) 125.60(15)	(B1,O1,O2,C5–C10) – (S1,C1–C4) = 10.40(8) (B2,O3,O4,C11–C16) – (S1,C1–C4) = 1.35(9)
1–2F	B(1)–F(1) 1.425(3) B(1)–O(2) 1.492(3) B(1)–O(1) 1.505(3) B(1)–C(1) 1.599(3) B(2)–F(2) 1.423(2) B(2)–O(4) 1.496(2) B(2)–O(3) 1.503(3) B(2)–C(4) 1.600(3)	F(1)–B(1)–O(2) 108.78(16) F(1)–B(1)–O(1) 107.98(16) O(2)–B(1)–O(1) 104.57(16) F(1)–B(1)–C(1) 110.01(17) O(2)–B(1)–C(1) 112.02(17) O(1)–B(1)–C(1) 113.23(16) F(2)–B(2)–O(4) 108.48(15) F(2)–B(2)–O(3) 108.46(15) O(4)–B(2)–O(3) 104.32(15) F(2)–B(2)–C(4) 110.47(16) O(4)–B(2)–C(4) 112.47(15) O(3)–B(2)–C(4) 112.36(16)	

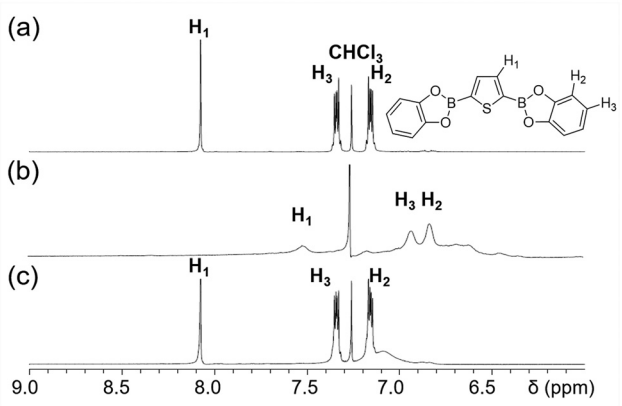

Fig. 3 ^{1}H NMR spectra ($CDCl_3$) of (a) **1** (20 mM); (b) **1** (20 mM) and *n*$BuNH_2$ (40 mM); and (c) **1** (20 mM), *n*$BuNH_2$ (40 mM) and TFA (80 mM).

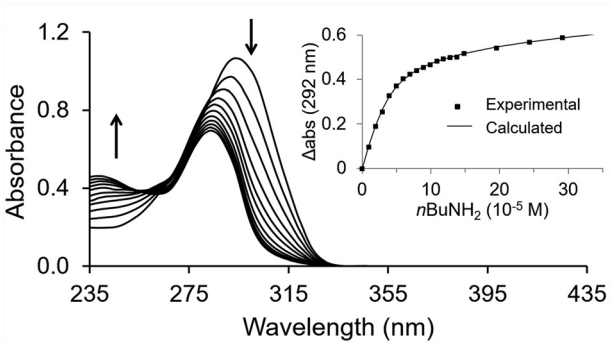

Fig. 4 Changes in the absorption spectra of **1** (35 μM in CH_2Cl_2) upon sequential addition of *n*$BuNH_2$. Inset: binding isotherm calculated at 292 nm.

cing the shielding effect from the partial negative charge generated at the boron centres. Significantly, the Lewis acid–base interaction was completely reversible. Upon the addition of excess trifluoroacetic acid (TFA), to protonate the *n*$BuNH_2$, the aromatic resonances shifted back to the original chemical shift of **1** (Fig. 3c). This reversibility indicated that **1** was stable both when amine was bound and under strongly acidic conditions.

Amine binding

To further evaluate the interactions between our bis(dioxaborole)s and amine analytes, *n*$BuNH_2$ was sequentially added, causing a decrease in the intensity and blue-shift in the absorption maximum of **1** from 292 nm to 283 nm (Fig. 4). This spectral change indicated that when **1** binds *n*$BuNH_2$, pi-conjugation was disrupted as the bis(dioxaborole) was forced to deviate from planarity, as observed in **1**-F (Fig. 2b). Two unique isosbestic points are observed as our ditopic Lewis acid **1** binds to the added amine. The first occurrence is at 283 nm and correlates with binding at the first boron. The second isosbestic point is observed at 253 nm as amine binds to the second boron center, though with a markedly lower affinity.

Using absorption titration data, binding constants were calculated based on a 1 : 2 host to guest binding stoichiometry[46] for amine guests binding to bis(dioxaborole)s **1**–**4** (eqn (1)). Herein, the change in absorbance is used to calculate binding constants *via* a nonlinear regression analysis, where b is pathlength, ε is absorptivity, and S is the total concentration of the substrate.[47] (ref Connors) The inset in Fig. 4 graphically depicts the spectral changes observed upon binding of *n*-butyl amine to bis(dioxaborole) **1**. The binding affinity for the second amine equivalent was less than that of the first (*e.g.* **1**: *n*$BuNH_2$, $\log K_{a1} = 5.10 \pm 0.12$ and $\log K_{a2} = 3.28 \pm 0.16$).

$$\frac{\Delta A}{b} = \frac{S(K_{a1}\Delta\varepsilon_{11}[L] + K_{a1}K_{a2}\Delta\varepsilon_{12}[L]^2)}{1 + K_{a1}[L] + K_{a1}K_{a2}[L]^2} \quad (1)$$

Compounds **1**–**4**, each having boron centres of differing Lewis acidity and/or steric demands, were used to explore how

Table 2 Calculated electron density surface and electrostatic positive potentials of **1–4** by DFT (B3LYP 6-31G*)

Compound	Electrostatic density surface[a] (−100–100 kJ mol^{-1})	Electrostatic potential at boron[b]
1 (–H)	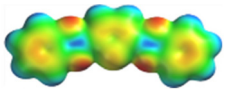	77.9 kJ mol^{-1}
2 (–CO_2Et)	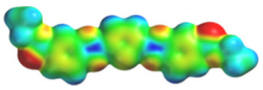	100.9 kJ mol^{-1}
3 (–OMe)	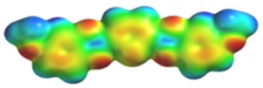	69.0 kJ mol^{-1}
4 (–di-*t*Bu)	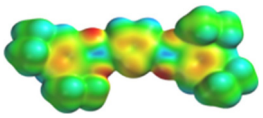	69.0 kJ mol^{-1}

[a] Red represents electron rich and blue represents electron deficient areas. [b] Larger numbers represent higher electron deficiency at boron.

these factors impact amine binding. Table 2 shows electron density maps and the positive electrostatic potential at boron for **1–4**. Moreover, low molecular weight amines with contrasting basicity and steric demand were chosen to examine the impact of these factors, including: *n*-butylamine (*n*BuNH$_2$, pK_b = 3.41), isopropylamine (iPrNH$_2$, pK_b = 3.37), diisopropylamine (iPr$_2$NH, pK_b = 2.95), and *N*-ethyldiisopropylamine (iPr$_2$EtN, pK_b = 2.60).[48,49] Compounds **1** (–H) and **2** (–CO_2Et) were employed to evaluate the influence Lewis acidity has on analyte binding, with **2** being more Lewis acidic (Table 2) as a result of the electron withdrawing esters. Consequently, Fig. 5 depicts **2** consistently displaying higher binding affinity for each amine compared to **1** due to this enhanced Lewis acidity.

Amine binding to **3** (–OMe) and **4** (–di-*t*Bu) was used to assess the impact of sterics on bis(dioxaborole)s binding Lewis bases. While the Lewis acidity is the same for these compounds, based on the calculated electrostatic potential at boron (Table 2), there are significant steric interactions around the boron centres in **4**, attributed to the 3-*t*-butyl group, that are not found in **3**. As a result, **3** exhibited higher affinity towards each analyte compared to **4**. Still, the exact role sterics play in diminishing binding in **4** is unclear. We postulate that the 3-*t*-butyl groups may either block access to the boron binding sites or introduce angle strain that reduces the change in the bond angles around the boron centers.

The sterics and basicity of the amine analytes also impact the binding affinity at boron. For example, while *n*BuNH$_2$ and iPrNH$_2$ exhibit similar basicity, the strength of the binding interactions with compounds **1–4** differs significantly due to the greater steric bulk of iPrNH$_2$ (Fig. 5). Interestingly, boronates **1–3** displayed higher binding affinity for iPr$_2$EtN compared to the other analytes studied, although the steric hindrance in iPr$_2$EtN was greater. This apparent anomaly is attributed to the stronger Lewis basicity of iPr$_2$EtN compared to the other amines. Still, these are competing factors and there is a point where basicity cannot overcome sterics. As observed for **4**, the affinity for iPr$_2$EtN is lower than that for *n*BuNH$_2$, and it appears that the significance of the steric interactions, in this case, outweigh the basicity effects.

While all the bis(dioxaborole)s studied bound each amine cross-reactively, each exhibited different binding patterns, providing a unique array of responses from **1–4** for each analyte. Fig. 6 shows the relative change in absorbance for **1–4** in response to the addition of analyte. Compound **2** consistently had the largest response to each analyte because it is the strongest Lewis acid. As a result, the response from **2** had minimal differentiation-ability between analytes (max fold-change = 1.3), and thus lacked selectivity based on amine basicity and sterics.

In contrast, the crowded and weak Lewis acid **4**, showed a small response to the bulky amines, yet exhibited a relatively strong response to the compact *n*BuNH$_2$, thereby displaying

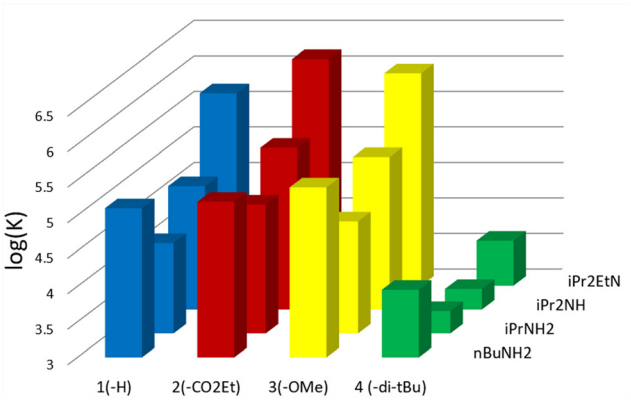

Fig. 5 Binding constants for the first equivalent of analyte bound (K_{a1}) determined from a 2 : 1 binding fit of absorption titration data at **1** (292 nm), **2** (299 nm), **3** (307 nm) and **4** (297 nm). Error bars are not shown, however, relative % standard deviation ranged from 0.5% to 5% with an average of 2.0%.

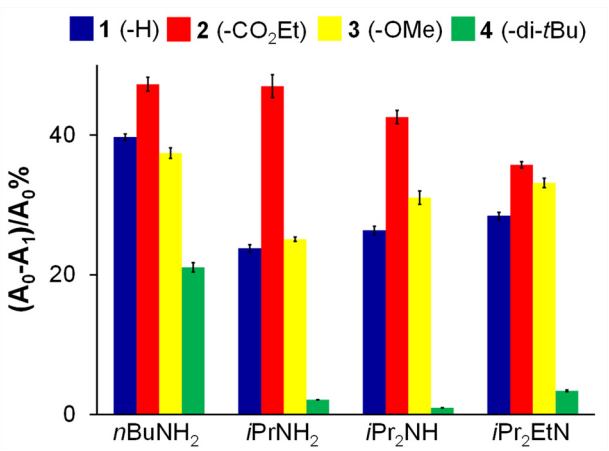

Fig. 6 Relative percent change in absorbance for **1–4** upon the addition of each amine (2 equiv.) creating distinct patterns.

clear selectivity (max fold-change = 22). Compounds **1** and **3** were cross-reactive towards binding these amines. Both exhibited similar affinity trends, with the responses determined by the electronic and steric properties of the amines.

Modelling of the electrostatic positive potentials at the unbound boron centre in each sensor-analyte complex (Table 3), suggests that the Lewis acidity and accessibility of the second sp^2 boron centre in each complex is significantly influenced by the first step binding. The second step binding constants, K_{a2} (Table S2) were also obtained from absorption titration studies, and are all smaller than the K_{a1} as expected due to electronics and binding statistics.

The interaction parameter, α (eqn (2)), is used to describe the interactions between ligands bound to multiple sites. In the case where two binding sites on the molecule are identical and exhibit no cooperativity, $K_{a1} = 4K_{a2}$ and $\alpha = 1$. In cases where binding of the ligand to one site affects the potential to bind to the other site, $\alpha > 1$ would indicate positive cooperativity, while $\alpha < 1$ will indicate negative cooperativity.

$$\alpha = \frac{4K_{a2}}{K_{a1}} \quad (2)$$

For the interaction between **1** and nBuNH$_2$, the interaction parameter, α, was found to be 0.060, indicating strong negative cooperativity. Comparatively, the stronger acids **2** and **3**, gave values of α = 0.053 and 0.039, respectively indicating very strong negative cooperativity due to the deactivation of the electron withdrawing groups with the addition of the nucleophile. Finally, compound **4** gave a value of α = 0.43, indicating weak negative cooperativity due to electron donation from the *t*-butyl groups and steric interactions impacting binding. Similar trends in interaction parameters were observed upon binding to the other amines (Table S3). These trends display effective communication from one boron site to the other through the thiophene linker, with this effect being more influential in molecules that contain an electron withdrawing group.

Table 3 Calculated electron density surface and electrostatic positive potentials of methylamine(MeNH$_2$)-sensor complex by DFT (B3LYP 6-31G*)

Compound	Electrostatic density surface[a] (−100–100 kJ mol^{-1})	Electrostatic potential at boron[b]
MeNH$_2$-**1** (–H)	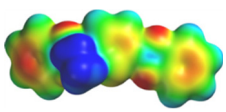	58.0 kJ mol^{-1}
MeNH$_2$-**2** (–CO$_2$Et)	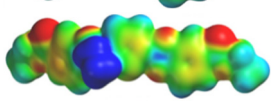	79.2 kJ mol^{-1}
MeNH$_2$-**3** (–OMe)	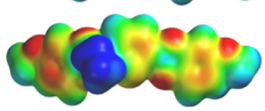	27.8 kJ mol^{-1}
MeNH$_2$-**4** (–di-*t*Bu)	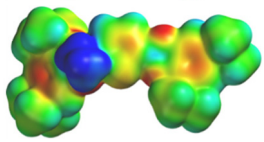	54.6 kJ mol^{-1}

[a] Red represents electron rich and blue represents electron deficient areas. [b] Larger numbers represent higher electron deficiency at boron.

Conclusions

In summary, Lewis acidic bis(dioxaborole)s **1–4** respond differentially to diverse Lewis bases, binding reversibly without ester hydrolysis. Binding affinity was affected by the Lewis acidity and sterics of the receptors, as well as by the Lewis basicity and sterics of the guests. Strong Lewis acids (*e.g.* **2**) had the highest binding affinity but poor selectivity, while crowded, weak Lewis acids (*e.g.* **4**) had low affinity but good selectivity. Bis(dioxaborole)s **1–4** each bound to all amines studied, though to varying degrees. This cross-reactivity can afford unique response patterns. We are currently focused on expanding the scope and utility of this work by using multiple responses from an array of bis(dioxaborole)s to identify environmentally relevant amines.

Author contributions

Li: conceptualization, investigation, and writing original draft; Boyt: writing – review & editing, cooperativity analysis; Cai: investigation & writing; Sloope: computational analyses; Lackovic: cooperativity analysis, review & revisions; Smith: crystallographic analyses; Lavigne: supervision and resources.

Conflicts of interest

The authors declare no conflict of interest.

Data availability

Supplementary data associated with this article has been included in the SI. Requests for additional details may be directed to the corresponding author.

Crystallographic data for **1** and **1**-2F have been deposited at the CCDC under accession numbers 1010916 and 1010917, respectively.[50a,b]

Acknowledgements

We thank the National Science Foundation (CHE-0718877) for financial support.

References

1 F. J. Green, *The Sigma-Aldrich Handbook of Stains, Dyes and Indicators*, Aldrich Chemical Company, Milwaukee, 1990.

2 S. W. Thomas, G. D. Joly and T. M. Swager, *Chem. Rev.*, 2007, **107**, 1339–1386.
3 J. Yang, Z. Y. Zhao, S. Wang, Y. L. Guo and Y. Q. Liu, *Chem*, 2018, **4**, 2748–2785.
4 S. Y. Lee, Y. Yu, J. B. Heo, J. A. Prayogo, D. R. Whang, H. Ahn, H. Yoo, B. H. Lee, S. Chung, K. Cho, J. Kim, D. W. Kang, H. Choi, J. W. Yoon and D. W. Chang, *ACS Appl. Mater. Interfaces*, 2025, **17**, 48574–48583.
5 T. Sutradhar and A. Misra, *J. Phys. Chem. A*, 2018, **122**, 4111–4120.
6 M. Cai, S. L. Daniel and J. J. Lavigne, *Chem. Commun.*, 2013, **49**, 6504–6506.
7 W. J. Niu, M. D. Smith and J. J. Lavigne, *J. Am. Chem. Soc.*, 2006, **128**, 16466–16467.
8 S. Muhammad, A. Khalid, S. Urrehman, S. Bibi, S. Riaz, S. S. Alarfaji, A. G. Al-Sehemi and A. R. Chaudhry, *Opt. Mater.*, 2024, **150**, 115253.
9 G. Turkoglu, M. E. Cinar and T. Ozturk, *Molecules*, 2017, **22**, 1522.
10 T. Gao, E. S. Tillman and N. S. Lewis, *Chem. Mater.*, 2005, **17**, 2904–2911.
11 G. J. Mohr, C. Demuth and U. E. Spichiger-Keller, *Anal. Chem.*, 1998, **70**, 3868–3873.
12 L. Bunková, F. Bunka, G. Mantlová, A. Cablová, I. Sedlácek, P. Svec, V. Pachlová and S. Krácmar, *Food Microbiol.*, 2010, **27**, 880–888.
13 Q. Zhang, L. Yu, W. Han, L. Yang, H. Li, S. Sun and Y. Xu, *Adv. Funct. Mater.*, 2024, **34**(51), 2410000.
14 R. S. Andre, L. A. Mercante, M. H. M. Facure, R. C. Sanfelice, L. Fugikawa-Santos, T. M. Swager and D. S. Correa, *ACS Sens.*, 2022, **7**, 2104–2131.
15 L. Prester, *Food Addit. Contam.,: Part A*, 2011, **28**, 1547–1560.
16 G. Preti, J. N. Labows, J. G. Kostelc, S. Aldinger and R. Daniele, *J. Chromatogr., Biomed. Appl.*, 1988, **432**, 1–11.
17 A. G. Kumbhar, S. V. Narasimhan and P. K. Mathur, *Anal. Chim. Acta*, 1994, **294**, 103–111.
18 H. Kataoka, *J. Chromatogr. A*, 1996, **733**, 19–34.
19 Q. Zhou, G. Jiang, J. Liu and Y. Cai, *Anal. Chim. Acta*, 2004, **509**, 55–62.
20 K. Fujita, T. Nagatsu, K. Shinpo, K. Maruta, R. Teradaira and M. Nakamura, *Clin. Chem.*, 1980, **26**, 1577–1582.
21 M. S. Maynor, T. L. Nelson, C. O'Sullivan and J. J. Lavigne, *Org. Lett.*, 2007, **9**, 3217–3220.
22 A. Satrijo and T. M. Swager, *J. Am. Chem. Soc.*, 2007, **129**, 16020–16028.
23 T. L. Nelson, C. O'Sullivan, N. T. Greene, M. S. Maynor and J. J. Lavigne, *J. Am. Chem. Soc.*, 2006, **128**, 5640–5641.
24 Y. M. Chung, B. Raman and K. H. Ahn, *Tetrahedron*, 2006, **62**, 11645–11651.
25 Y. K. Che, X. M. Yang, S. Loser and L. Zang, *Nano Lett.*, 2008, **8**, 2219–2223.
26 M. R. Ajayakumar and P. Mukhopadhyay, *Chem. Commun.*, 2009, 3702–3704.
27 H. Y. Xia, T. H. Liu, L. N. Gao, L. K. Yan and J. W. Wu, *Appl. Surf. Sci.*, 2011, **258**, 254–259.
28 S. Yamaguchi, S. Akiyama and K. Tamao, *J. Am. Chem. Soc.*, 2001, **123**, 11372–11375.
29 A. Sundararaman, K. Venkatasubbaiah, M. Victor, L. N. Zakharov, A. L. Rheingold and F. Jäkle, *J. Am. Chem. Soc.*, 2006, **128**, 16554–16565.
30 G. Zhou, M. Baumgarten and K. Müllen, *J. Am. Chem. Soc.*, 2008, **130**, 12477–12484.
31 W. J. Liu, M. Pink and D. Lee, *J. Am. Chem. Soc.*, 2009, **131**, 8703–8707.
32 W. Niu, B. Rambo, M. D. Smith and J. J. Lavigne, *Chem. Commun.*, 2005, 5166–5168.
33 J. K. Day, C. Bresner, N. D. Coombs, I. A. Fallis, L.-L. Ooi and S. Aldridge, *Inorg. Chem.*, 2008, **47**, 793–804.
34 A. Oehlke, A. A. Auer, I. Jahre, B. Walfort, T. Rueffer, P. Zoufala, H. Lang and S. Spange, *J. Org. Chem.*, 2007, **72**, 4328–4339.
35 T. Neumann, Y. Dienes and T. Baumgartner, *Org. Lett.*, 2006, **8**, 495–497.
36 E. Sheepwash, N. Luisier, M. R. Krause, S. Noé, S. Kubik and K. Severin, *Chem. Commun.*, 2012, **48**, 7808–7810.
37 K. Song, W. J. Ye, X. C. Gao, H. G. Fang, Y. Q. Zhang, Q. Zhang, X. L. Li, S. Z. Yang, H. B. Wei and Y. S. Ding, *Mater. Horiz.*, 2021, **8**, 216–223.
38 G. W. Kabalka, N. K. Reddy and C. Narayana, *Tetrahedron Lett.*, 1992, **33**, 865–866.
39 L. Weber, D. Eickhoff, V. Werner, L. Boehling, S. Schwedler, A. Chrostowska, A. Dargelos, M. Maciejczyk, H.-G. Stammler and B. Neumann, *Dalton Trans.*, 2011, **40**, 4434–4446.
40 Mole ratio plots provided a biding stoichiometry of 1 : 1.93.
41 No signals were observed for the thiophene diboronic acid when mixed with catechol in $CDCl_3$ (Fig. 1c) because the diboronic acid readily forms anhydrides and precipitates from solution.
42 The peak present in each ^{11}B NMR spectra at 19.3 ppm is from boric acid. $BF_3{\cdot}Et_2O$ was used as an external reference at 0 ppm. Boric acid was used as an internal reference (in a capillary tube in NMR tube) at 19.3 ppm and does not interact with sample.
43 J. F. Blount, P. Finocchiaro, D. Gust and K. Mislow, *J. Am. Chem. Soc.*, 1973, **95**, 7019–7029.
44 A. Nagai, T. Murakami, Y. Nagata, K. Kokado and Y. Chujo, *Macromolecules*, 2009, **42**, 7217–7220.
45 Z. Yuan, N. J. Taylor, R. Ramachandran and T. B. Marder, *Appl. Organomet. Chem.*, 1996, **10**, 305–316.
46 W. Al-Soufi, P. R. Cabrer, A. Jover, R. M. Budal and J. V. Tato, *Steroids*, 2003, **68**, 43–53.
47 K. Connors, *Binding Constants: the measurement of molecular complex stability*, Wiley, New York, 1987.
48 H. K. Hall Jr., *J. Am. Chem. Soc.*, 1957, **79**, 5441–5444.
49 *Determination of Organic Structures by Physical Methods*, ed. E. A. Braude and F. C. Nachod, 1955.
50 (*a*) CCDC 1010916: Experimental Crystal Structure Determination, 2026, DOI: 10.5517/ccdc.csd.cc12xy64; (*b*) CCDC 1010917: Experimental Crystal Structure Determination, 2026, DOI: 10.5517/ccdc.csd.cc12xy75.